

Dalton Transactions

Accepted Manuscript



This is an *Accepted Manuscript*, which has been through the Royal Society of Chemistry peer review process and has been accepted for publication.

Accepted Manuscripts are published online shortly after acceptance, before technical editing, formatting and proof reading. Using this free service, authors can make their results available to the community, in citable form, before we publish the edited article. We will replace this *Accepted Manuscript* with the edited and formatted *Advance Article* as soon as it is available.

You can find more information about *Accepted Manuscripts* in the [Information for Authors](#).

Please note that technical editing may introduce minor changes to the text and/or graphics, which may alter content. The journal's standard [Terms & Conditions](#) and the [Ethical guidelines](#) still apply. In no event shall the Royal Society of Chemistry be held responsible for any errors or omissions in this *Accepted Manuscript* or any consequences arising from the use of any information it contains.

Zeolite films as building blocks for antireflective coatings and vapor responsive Bragg stacks

Tsvetanka Babeva^{1,*}, Hussein Awala^{2,*}, Marina Vasileva¹, Jaafar El Fallah², Katerina Lazarova¹, Sebastien Thomas², and Svetlana Mintova^{2,*}

¹Institute of Optical Materials and Technologies “Acad. J. Malinowski”, Bulgarian Academy of Sciences, Acad. G. Bonchev str., bl. 109, 1113 Sofia, Bulgaria

²LCS, ENSICAEN, CNRS, University of Caen, 6, boulevard du Maréchal Juin, 14050 Caen Cedex, France

*These authors contributed equally to this work as first author.

Abstract

Zeolite films (LTL, BEA and MFI) are prepared with a thickness in the range 50-170 nm through multistep spin-on deposition method. The optical properties of the zeolite films including refractive index, extinction coefficient and thickness are determined from the reflectance spectra using nonlinear curve fitting method. The total free pore volume of the films using the Bruggeman effective medium theory is calculated. The potential of the zeolite films for broadband antireflection (AR) application is demonstrated. Five times reduction of the reflectance of silicon substrate covered with the double AR films comprising of MFI type zeolite (120 nm) deposited on Nb₂O₅ (60 nm) is achieved. Additionally, the MFI zeolite film is used as a building block of vapor responsive Bragg stacks with a strong response towards acetone. The reversible response of the Bragg stacks towards acetone without additional annealing opens up the possibility to prepare sensors with optical read-out by incorporation of sensitive and transducer elements in a single device.

Keywords: zeolites, films, optical properties, effective medium approximation, antireflective coatings, sensors.

1. Introduction

Zeolites (molecular sieves) are crystalline materials with framework-type structures built of regular and uniform pores of molecular dimensions.¹ The zeolites are classified according to their framework type, pore dimension and the Si/Al ratio of the frameworks.

The high crystalline zeolites have found wide application in catalysis, separation, and ion exchange processes.²⁻⁶ In addition to the traditional uses, advanced applications of these materials have also been explored.⁷ Recent developments of synthesis procedures for zeolite nanocrystals and their arrangements in thin-to-thick films, membranes and hierarchical bodies have pushed them into new, diverse and economically significant applications that have not been recognized before such as low dielectric constant (low-k) zeolite film used as insulator for computer chips,⁸⁻¹¹ antireflective coatings,¹² antimicrobial coatings,¹³ corrosion-resistant coatings for aerospace alloys,¹³ flexible and transparent moisture getter films,¹⁴ various sensor devices,¹⁵⁻¹⁷ etc. Besides, the unique combination of chemical and optical properties of zeolites opened up the possibility of using them as part of tunable Bragg stacks.¹⁸⁻²³ The porous Bragg stacks are considered for chemical sensing application with optical encoding. The idea behind is the change of refractive index and/or thickness of the layers in the Bragg stack due to ion-exchange, sorption, and capillary condensation of molecules adsorbed in the pores, which result in a shift of the high reflectance band and consequent change of their color.

A number of novel applications of zeolites depend on the ability to create thin, adhesive films on various substrates.⁷ Various techniques were developed for the fabrication of zeolite-based devices such as direct synthesis of zeolite crystals on a support, seed methods and attachment of crystals on functionalized surfaces.^{7,24,25} Besides a spin coating method for deposition of zeolite films is widely applied.^{9,26} Spin-on process is simple, fast and offers operating precision, flexibility and high uniformity over different surfaces. Moreover, spin coating of colloidal suspensions of nanosized zeolites offers the possibility to form smooth layers on almost all kinds of surface with and without surface modification. Also, spin coating allows effective control of film thicknesses by varying the concentration of suspensions and the spin-on rotation rates.^{26,27}

Reliable and non-destructive measurements of zeolite film characteristics such as the film thickness and refractive index (or dielectric constant) are beneficial for estimating the performance of zeolite films in the above-mentioned applications. It has been confirmed that the deposition parameters such as the concentration of coating suspensions, number of coating steps, speed of deposition, as well as the type of binders, had a pronounced influence on the thickness, mechanical, and optical properties of the films.²⁸ If the optical properties of zeolite films can be controlled then numerous opportunity for their practical applications will be opened up.

In this paper the optical properties of zeolite films obtained by spin coating of aqueous zeolite suspension consisting of nanocrystals with different framework type structures and chemical composition are studied. Besides, the possibility of controlling the optical thickness of the zeolite films through multi-step spin coating deposition is investigated. A color chart for fast and reliable determination of the thickness of zeolite films based on their optical properties is suggested. The application of zeolite films as single and double layer antireflection coatings (AR) for silicon substrate is demonstrated along with their implementation as sensitive elements in vapor responsive Bragg stacks.

2. Experimental

2.1 Preparation and characterization of nanosized zeolites

Stable coating suspensions of discrete nanosized zeolites (LTL and BEA-framework types) from colloidal precursor suspensions under hydrothermal conditions are prepared according to the procedures described elsewhere.^{29,30} The as-prepared precursor suspensions for BEA and LTL type zeolites were aged at room temperature for 24 hours prior to treatment at 100 °C for 3 days and 170 °C for 18 hours, respectively. Additionally, pure silica MFI-type zeolite (Si-MFI) was synthesized according to the procedure described before; the synthesis was performed at 90 °C for 3 days.³¹ After the hydrothermal treatment, the zeolite nanoparticles were purified by two steps centrifugation (24,500 rpm, 1 h) and redispersed in double distilled water.

The chemical composition of the samples was determined by inductively coupled plasma (ICP) optical emission spectroscopy using a Varian ICP-OES 720-ES. The Si/Al ratio for Si-MFI, BEA, and LTL type zeolites is equal to ∞ , 14 and 3.6, respectively.

The size of the nanoparticles was measured by Dynamic light scattering (DLS) using a Malvern Zetasizer Nano. The size and crystallinity of the zeolite crystals were also confirmed by Transmission Electron Microscopy (TEM) using a JEOL 2010 FEG operating at 200 kV. Additionally, the surface charge of the crystals was determined by measuring the zeta potential value of suspensions at a constant solid concentration (1 wt. %) and pH=8.5.

The crystallinity of the Si-MFI, BEA and LTL powder samples was proven by X-ray diffraction (XRD) analyses carried out with *PANalytical* X'Pert Pro diffractometer with $\text{CuK}\alpha$ monochromatized radiation ($\lambda = 1.5418 \text{ \AA}$). Additionally, the moisture content and stability of the samples after calcination (550 °C) was investigated through Thermogravimetric analysis (TGA) using SETSYS instrument (SETARAM) analyzer (heating rate of $5 \text{ }^\circ\text{C min}^{-1}$ under 40 ml.min^{-1} flow of air).

2.2 Preparation and characterization of zeolite films

The zeolite films were prepared by spin coating approach: 0.25 ml of aqueous colloidal suspensions with a constant concentration (1 wt. %) was mixed with 0.05 ml of methylcellulose and the mixture was dropped onto preliminarily cleaned Si-substrate according to the procedure described.³² The speed and duration of the spinning rotation were 2500 min^{-1} and 30 s, respectively. In order to obtain thicker films, the coating procedure was repeated 2-to-5 times. The layers were annealed at 320 °C for 30 minutes with temperature acceleration of $10 \text{ }^\circ\text{C/min}$ after each deposition step. The zeolite films prepared have a thickness in the range 50-170 nm (selected samples were subjected to characterization).

The homogeneity, crystal morphology and thickness of the films were studied by Scanning Electron Microscopy (SEM) using JEOS JSM6700F SEM at an accelerating voltage 30.0 kV. Reflectance spectra (R) of zeolite films deposited on silicon substrates were measured in the spectral range 400 – 900 nm using UV-VIS-NIR spectrophotometer (Cary 5E, Varian) with an accuracy of 0.3 %. Refractive index (n), extinction coefficient (k), and thickness (d), of the films were determined simultaneously from the reflectance measurement using non-linear curve fitting method described in details elsewhere.²³ The experimental errors for n , k and d are 0.005, 0.003 and 2 nm, respectively.

3. Results and discussion

3.1 Zeolite nanocrystals assembled in thin films

The DLS and TEM results for zeolite suspensions with Si-MFI, BEA and LTL type nanocrystals are presented in Fig. 1. As can be seen, the mean hydrodynamic diameter of the zeolites is almost the same, i.e., 35 nm for Si-MFI and 45 nm for both the BEA and LTL- type crystals. In addition to the size, the morphology of the zeolites is revealed by TEM. The Si-MFI and BEA crystals are almost spherical in shape, and the latest is build of interconnected nanocrystals forming aggregates. Only the LTL crystals exhibit rectangular shape with well-developed sharp edges (Fig. 1). The high degree of crystallinity of the three type zeolites is confirmed by the XRD. The typical Bragg peaks for MFI, BEA and LTL type crystalline structures are present in the patterns (Fig. 2), and only a broadening of the peaks due to the small particle size of the crystallites is observed.³³

The zeolite nanocrystals are deposited in the films (thickness of 50-170 nm) by spin coating with several deposition steps. The three type films with a constant thickness of 70 and 150 nm are presented in Fig. 3. As shown, the zeolite nanocrystals are closely packed and form continuous films along the silicon substrates. The quality of the zeolite films (surface roughness and homogeneity) is preserved in the entire thickness range under investigation (50-170 nm).

The optical properties of the films are determined based on the reflectance spectra recorded for Si-MFI, LTL and BEA zeolite films. A decrease of reflectance (R) with increasing the films thickness is observed for all samples (Fig. 4). The changes of R for LTL films are the strongest while for the Si-MFI films are the weakest. When the thickness of the films increases approximately from 70 nm to 170 nm, the R -value decreases with 12, 16 and 20 % for Si-MFI, BEA and LTL-type films, respectively (data are taken at wavelength of 900 nm). Considering that R is a function of the optical thickness (combining both the refractive index and physical thickness) of the films, the assumption could be made that the biggest change of R for the LTL film is due to the higher refractive index of the zeolite crystals as compared to others.

Using the reflectance spectra, the refractive index, extinction coefficient and thickness of the films are calculated.²³ Figure 5 presents the refractive index of zeolite films with a thickness of 100 nm as a function of the wavelength, i.e. the dispersion curves of n . As can be seen, the dispersion of n is very weak that is not surprising considering that the zeolite films are transparent in the studied spectral range. The smallest value of n for the Si-MFI film ($n = 1.172$) and the highest value for the LTL film ($n = 1.362$) are obtained, while the n value of BEA is in the middle ($n = 1.296$). The values of n for Si-MFI films obtained in this study are in a good agreement with the results reported before.³³

To check how the different chemical compositions of zeolites (Si/Al = ∞ , 14, 3.6) influence the refractive index of the films, we calculate the n curves for mixtures of SiO₂ and Al₂O₃ with volume fractions corresponding to the Si/Al ratio of the zeolites. Purposely the Bruggeman effective medium theory is used.³⁴ The idea is to regard the mixture from silica and alumina as a medium with effective optical properties that depend on the refractive index and volume fractions of the two phases present:^{35,36}

$$f_1 \frac{\varepsilon_1 - \varepsilon_e}{\varepsilon_1 + 2\varepsilon_e} + f_2 \frac{\varepsilon_2 - \varepsilon_e}{\varepsilon_2 + 2\varepsilon_e} = 0; \quad f_1 + f_2 = 1, \quad (1)$$

where ε_1 , ε_2 and ε_e are dielectric constants ($\varepsilon = n^2$) of SiO₂, Al₂O₃ and a mixture, respectively, while f_1 and f_2 are the volume fractions of SiO₂ and Al₂O₃ phases. Knowing that the Si/Al ratio is 3.6 for LTL and 14 for BEA, the f_1 and f_2 are calculated to be 0.78 and 0.22 for Si/Al = 3.6, and 0.933 and 0.067 for Si/Al = 14. In order to calculate the effective dielectric constants ε_e using Eq. 1, the effective dielectric constants ε_1 and ε_2 of the two phases presented in the mixture, i.e., for SiO₂ and Al₂O₃ are required. The refractive index spectra for SiO₂ and Al₂O₃ are taken from Ref. 37 and presented in Figure 5 d, g. For clarity, it is important to note that the two parameters ε and n are related as follows $\varepsilon = n^2$. The calculations concerning effective medium approximations are performed using dielectric constants, but the results in the figures are presented as refractive index values in order to compare with already published data.

The effective dielectric constants ϵ_e for media with different Si/Al ratio are calculated by means of Eq. 1 using the already calculated values of f_1 and f_2 for SiO₂ and Al₂O₃³⁷ (Fig. 5 d, g). The effective refractive indices for different media with a ratio of Si/Al=14 (curve e) and Si/Al=3.6 (curve f) are presented in Fig. 5. It is seen that the increase of the Al₂O₃ fraction in the mixture leads to the increase of the refractive index of the effective media, i.e., $n = 1.458, 1.471$ and 1.501 for pure SiO₂ and mixtures with SiO₂ : Al₂O₃ equal to 14 and 3.6, respectively. Therefore one possible explanation for the higher refractive index of LTL and BEA films as compared to the Si-MFI film is the different chemical composition of the zeolites, i.e., the presence of Al.

Besides, the volume fraction of the free pores in the zeolite film, which is a measure of the total porosity, is calculated using Eq. 1,^{35,36}. In this case the zeolite film is regarded as an effective medium built of two phases, i.e., SiO₂:Al₂O₃ and air. The already calculated refractive indices of the zeolites (n_e) (Fig. 5 a, b, c) are regarded as effective dielectric constants $\epsilon_e = n_e^2$. The data for SiO₂ (curve d) along with the calculated values for Si/Al=14 (curve e) and Si/Al=3.6 (curve f) are used for determination of ϵ_1 ; the second phase is air with $\epsilon_2 = 1$. The calculated free pore volume f_1 from Eq.1 of the Si-MFI, BEA and LTL films is 61, 37 and 27 %, respectively. In our previous study, the free pore volume of isolated Si-MFI nanocrystals was calculated to be 19 %.³⁵ In the current samples, the interparticle mesoporosity exists as seen in the SEM pictures (Fig. 3), and this explains the higher free pore volume of the zeolite films. Moreover, the interparticle space is very well seen in the Si-MFI film in comparison to the other two types. The most packed nanocrystals are observed in the LTL film, which explains the lower free pore volume together with the one-dimensional pore system of this material. Similar observation for MFI films are made by Wang et al.⁹ the films exhibit a bimodal pore size distribution consisting of micropores (0.55 nm) and interparticle mesopores (2.7–2.8 nm).

It is well known that the moisture has a significant influence on the n value of films. Considering the hydrophilic nature of BEA and LTL type zeolites, we can assume that the higher refractive index is due to the higher water content in the micro- and mesopores. If air with the refractive index of unity is substituted with water with a refractive index of 1.33, then the effective refractive index of the film will increase. The calculated reduced free pore volume for LTL and BEA films is in agreement with the hypothesis of

partly filled pores and lower mesoporosity (high packing of crystals). To confirm the assumption of different water content in the studied samples we have conducted thermogravimetric (TG) analysis of zeolite samples that were subjected to preliminary annealing (Fig. 6). As can be seen, the water content in Si-MFI zeolite is the smallest (the weight loss of 1.8 % is measured). Although no water is expected for pure silica MFI-type zeolite, the low content is due to the presence of many structural defects, which are more pronounced in the nanosized zeolites. The respective weight losses for the BEA and LTL-type zeolites are 10.6 % and 12.5 %, respectively, which correspond to the release of water below 200 °C. These results confirm the hypothesis made above that the higher values of n and the smaller free pore volumes for BEA and LTL thin films are mostly due to the water present in their pores. Figure 7 presents the dependence between the refractive index and the thickness of the Si-MFI, BEA and LTL films. It is important to mention that no special precautions for removing of water from the films were taken prior to the measurements of the refractive index. In the thickness region 70-120 nm, an increase of n is observed for all samples. A clear correlation between the water content in the zeolites and the change of the refractive index of the films is revealed by comparing the results presented in Figs. 6 and 7. The film thickness dependence of n is the strongest for the LTL film with the highest water content, while for the Si-MFI film is negligible.

For proper operation of devices using zeolite films, for example antireflective coatings or Bragg stacks, it is essential the optical thickness of the films to be known with high precision. Therefore, the reproducibility of deposition of zeolite films with controlled optical properties and thicknesses will contribute positively to the wider implementation of these materials as active or passive counterparts in different devices. The change of the films thickness as a function of the number of consecutive steps of deposition is shown in Fig. 8. For the preparation of the three types of films, the concentration of the coating colloidal suspensions was the same (1 wt. %). Besides the deposition conditions are kept the same: 0.3 ml coating suspension per layer, spinning rate 2500 min⁻¹, and deposition time 30 sec. After each deposition step the samples are subjected to annealing at 320 °C for 30 min in order to increase the mechanical stability of the films. The total thickness of 155, 120 and 115 nm is obtained for LTL, Si-MFI and BEA films after conducting the spin-on process five times. Interestingly after the first

deposition step the thickness for all films is almost the same (50 nm). This means that at fixed rotation speed the thickness of the single film depends mainly on the concentration of the zeolite nanoparticles in the coating suspensions.

The results from the optical characterization of zeolite films are averaged over measurements of three samples prepared at the same experimental conditions. The error bars in Figure 8 presents the overall error in thickness accounting for both the error that originates from the reflectance measurement inaccuracy and the reproducibility error. It is seen that the accuracy in thickness is high enough - the error in d is less than 3 %. The amount and concentration of coating suspension, spin-on rotation and substrate size should be the same for all experiments in order to reproduce the films with defined thickness.

Additional measurements not shown here reveal that the thickness of the films increases linearly with increasing the zeolite concentration in the coating suspensions. Thus three times higher thickness (around 150 nm) could be achieved in a single deposition step if the concentration of the zeolites is 3 wt. %. Another way to increase the thickness of the film is to reduce the spinning rate. However the quality of films obtained at lower spinning rates (1000 min^{-1}) slightly deteriorates. Simultaneously the increase of the thickness is less than two times (from 50 nm to 90 nm) when the rotation speed decreases from 2500 to 1000 min^{-1} . It is also seen that the rate of thickness growth is the highest for LTL film and almost the same for the BEA and Si-MFI films (Fig. 8). The main factors that influence the film thickness, such as concentration, particle sizes and rotation speed, are kept the same in these experiments. Therefore another parameter has to be considered that influences the film thickness. A possible reason for the observed differences in the films is the surface properties (hydrophilicity/hydrophobicity) and possibly the morphology of the individual zeolite crystals. Moreover, the morphology of the LTL crystals helps for the better packing resulting in higher thickness of the films (see Figs. 3 and 8).

Finally we present a simple method for determination of the thickness of zeolite films. The widely used method for fast determination of physical thickness of SiO_2 film in microelectronic is through a visual inspection of the color of SiO_2 film thermally grown on Si-substrates. At certain values of optical thickness (n, d) for the film, its

reflectance has a peak due to the constructive interference between the multiple reflected waves from the two boundaries of the film, and as a result the film becomes colored. Figure 9 shows pictures of the zeolite films deposited on Si-substrate with denoted thickness in the range 70-370 nm. It is seen that the color of the films changes starting from brown for the thinnest film to blue-green for the thickest one. The color chart of the thermally grown SiO₂ film is presented in Fig. 9 for comparison. It is generated using the results from Ref. 38 by choosing the type of the material (SiO₂), thickness range, substrate (Si), light source (daylight), and type of color presentation. It is seen that for thin zeolite films there is a very good match between the SiO₂ color chart and the color of the zeolite films. However for films with a thickness above 200 nm a divergence appears. The reason is the different refractive indices of SiO₂ (1.45) and zeolite films (1.15-1.35). On the basis of the calculated thicknesses and refractive index, a color chart for the zeolite films is generated using³⁸ (Fig. 9). In this case, instead of choosing SiO₂ material, a Sentech-Cauchy-Layer is taken with a refractive index $n_0=1.25$. Very good agreement between the color of the samples (Fig. 9 a) and the generated chart is obtained in the case of $n_0=1.25$. This color chart can be used for rapid and reliable control of the thickness of zeolite films deposited on silicon substrate.

3.2 Application of zeolite films

3.2.1 Antireflective coatings

Based on the comparison between the reflectance of zeolite films and silicon substrate, it is suggested that the single zeolite film could be used as antireflective (AR) coating for silicon substrate (Fig. 4). Figure 10 presents reflectance of Si-MFI, BEA and LTL zeolite films deposited on silicon substrate with thicknesses of 120, 115 and 110 nm, respectively. It is seen that the zeolite films have smaller reflectance compared to that of the bare silicon substrate. The zeolite AR coatings show significant decrease of reflectance (R): the average R changes from 34.3 % for bare silicon substrate to 23, 20.7 and 15.1 % for Si-MFI film (120 nm), BEA film (115 nm), and LTL film (110 nm), respectively. The smallest values of R measured are 21.2, 18.3 and 11.8% for Si-MFI, BEA and LTL AR coatings, respectively. Moreover, the biggest reduction in the R -value is achieved for the LTL zeolite film deposited on silicon substrate. The R -value decreases

from 48 % to 31 % at wavelength of 400 nm, from 35 % to 11.8 % at 600 nm, and from 32 % to 17.5 % at 800 nm (Fig. 10). In conclusion the use of zeolite films as antireflective coatings is clearly demonstrated.

Moreover, stacks consisting of alternating films with different refractive indices are required to decrease further the R-value. As low refractive index film, the Si-MFI was selected ($n=1.2$) (Fig. 7), which is favorable from the viewpoint of multilayered AR stacks.³⁹ As high refractive index film, the Nb₂O₅ was chosen ($n = 2.4 - 2.1$). The Nb₂O₅ film is obtained by a sol-gel method as explained in details elsewhere.⁴⁰ Briefly, the Nb sol was prepared by a sono-catalytic method using 0.400 g NbCl₅ (99 %, Aldrich), 8.3 ml ethanol (98 %, Sigma-Aldrich) and 0.17 ml distilled water. Instead of stirring, the solution was subjected to sonication for 30 min and aged for 24 h at ambient conditions prior to spin coating.⁴⁰ Thin Nb₂O₅ films were deposited by dropping of 0.3 ml of the coating solution on the substrate and annealing at 320 °C for 30 min. The required thicknesses of stack's films are determined through minimization of reflectance over wide spectral range using already calculated optical constants of both materials. The most appropriate design is experimentally implemented, and the reflectance of the stack's film is shown in Fig. 10 (curve f). The stack consists of 120 nm Si-MFI film deposited on the top of 60 nm Nb₂O₅ film on silicon substrate. The average reflectance of the AR coating is 7.1 %, which implies that 4.8 times of the silicon reflectance is reduced. The reflectance spectra of single Nb₂O₅ film with a thickness of 60 nm deposited on silicon substrate is also presented in Fig. 10 (curve e) for comparison. The average reflectance achieved for Nb₂O₅ AR coating is 9.9 %. Thus, the role of zeolite film deposited on the top of Nb₂O₅ film is clearly seen, and most pronouncedly at lower wavelengths.

3.2.2 Bragg stacks

Bragg stacks are multilayered systems comprising high and low refractive index materials with quarter-wave optical thicknesses ($nd = \lambda_c/4$, n -refractive index, d -physical thickness, λ_c -wavelength of incident light) arranged in periodic manner. Due to interference phenomena Bragg stacks exhibit band of high reflectance that is centered at λ_c , and it is highly sensitive to changes in optical thickness of the constituent films. If

sensitive materials are used as building blocks then the position of reflectance band can be controlled upon the influence of external stimuli.⁴¹

For the preparation of Bragg stacks an alternating spin coated sol-gel Nb₂O₅ and Si-MFI zeolite films with target thicknesses of 60 and 120 nm, respectively are used. The development of reflectance band with increasing the number of layers in the stack is studied by measuring the reflectance spectra (*R*) at normal incidence of unpolarized light for structures comprising 2, 3, 5 and 7 layers (Figure 11). In order to increase the *R-value* of the stacks, it is found that starting with Nb₂O₅ layer deposited on the glass substrate is beneficial; the *R-value* increases with the number of layers (Fig. 11), and reaches a value of 74 % for the seven-layers.

The adsorption and desorption of acetone for the stacks with different number of layers are carried out and the results are depicted in Figure 12. The transmittance signal (*S*) as a function of time was measured at wavelength of 400 nm, and these measurements are repeated for 3 cycles. As shown in Fig 12, both the adsorption and desorption branches comprise two clearly distinguishable processes (Fig. 12). A fast adsorption takes place more profoundly for sample with 7 layers, followed by steady state of the transmittance signal (*S*). After switching off the acetone vapor, a very fast desorption takes place. A recovery of the initial signal is observed within 5 min without additional annealing. The sensitivity of the stacks is increased from 1.8 % to 4.8 % and to 8.9 % for 3, 5 and 7- layers, respectively. The changes of the signal, which is the transmittance of reflectance, are associated with the changes in the effective refractive index of the stacks structures. Additional measurements of a single layer combine with the modeling of the measured spectra show that only the refractive index of the Si-MFI film changes when the structure is exposed to acetone vapors. This is regarded as an advantage because the selective behavior of zeolites could be fully explored. The exposure to acetone results in replacement of air inside the zeolite pores with acetone with higher refractive index. This leads to red shift of band edge and subsequent change of the measured signal at a fixed wavelength.

4. Conclusions

The optical properties of zeolite films obtained by spin coating of suspensions of Si-MFI, LTL and BEA nanocrystals are investigated. It is demonstrated that zeolite nanocrystals are closely packed and form continuous films that cover the entire surface of the silicon substrate. The optical characterization reveal that the Si-MFI film exhibits the smallest refractive index ($n = 1.172$), while the LTL film has the highest one ($n = 1.362$), while the value of n for BEA films is in the middle ($n = 1.296$). A correlation between different n values of the films and increased aluminum content in BEA and LTL type zeolites, and the different moisture content in the films was obtained. Besides it was demonstrated that the water content in the zeolite pores leads to a decrease of the free pore volume of the films, which are 61, 37 and 27 % for Si-MFI, BEA and LTL type films, respectively as calculated by Bruggeman effective medium theory. This confirms that the pores of the LTL and BEA films are partly filled with water. Besides, a zeolite color chart is suggested, that can be used for fast and reliable determination of the thickness of zeolite films deposited on silicon substrate with refractive index in the range 1.15-1.36.

The potential of zeolite films for the broadband antireflection (AR) application is demonstrated; single and double AR films on silicon substrate are prepared. Five times reduction of the reflectance is achieved for the double AR films comprising of Si-MFI (120 nm) deposited on top of Nb₂O₅ (60 nm). Moreover, the Si-MFI zeolite film is successfully used as building block of vapor responsive Bragg stack with strong response towards acetone. Besides, a fast recovery without additional annealing is observed that opens up the possibility for preparation of sensors with optical read-out by incorporation of the sensitive and the transducer elements in a single device.

The reproducibility of zeolite films preparation with controlled optical properties is demonstrated which are of significant importance for their wide implementation as active or passive counterparts in different devices.

Acknowledgements: The financial support from MEET, Materials for Energy Efficiency in Transport, INTERREG EC and Bilateral BAS-CNRS projects is acknowledged.

References

1. R. M. Barrer, *Hydrothermal Chemistry of Zeolites*, Academic Press, London, 1982.
2. J. Čejka, A. Corma and S. Zones, *Zeolites and Catalysis: Synthesis, Reactions and Applications*, New York, Wiley-VCH, 1st ed., 2010.
3. M. Guisnet and J.-P. Gilson, in *Zeolites for Cleaner Technologies*, eds. M. Guisnet, J.-P. Gilson, Imperial College Press, London, 2005, pp. 1–28.
4. G. J. d. A. A. Soler-Illia, C. Sanchez, B. Lebeau and J. Patarin, *Chem. Rev.*, 2002, **102**, 4093.
5. E. M. Flanigen, R. W. Broach and S. T. Wilson, in *Zeolites in Industrial Separation and Catalysis*, ed. S. Kulprathipanja, Wiley VCH, Weinheim, 2010, pp. 1–26.
6. A. Corma, *J. Catal.*, 2003, **216**, 298.
7. T. Bein and S. Mintova, *Stud Surf Sci Catal.*, 2005, **157**, 263.
8. Z. B. Wang, H. T. Wang, A. Mitra, L. M. Huang and Y. S. Yan, *Adv. Mater.*, 2001, **13**, 746.
9. Z. B. Wang, A. P. Mitra, H. T. Wang, L. M. Huang and Y. S. Yan, *Adv. Mater.*, 2001, **13**, 1463.
10. S. Mintova, M. Reinelt, T. H. Metzger, J. Senker and T. Bein, *Chem. Commun.*, 2003, **3**, 326.
11. A. Mitra, T. Cao, H. Wang, Z. Wang, L. Huang, S. Li, Z. Li and Y. Yan, *Ind. Eng. Chem. Res.*, 2004, **43**, 2946.
12. C.H. Chen, S-Yi Li, A.S.T. Chiang, A.T. Wu and Y.S. Sun, *Sol. Energ. Mat. Sol. C*, 2011, **95**, 1694.
13. Ch. M. Lew, Rui Cai and Y. Yan, *Accounts Chem. Res.*, 2010, **43**, 210.
14. C.S. Wu, J-Yu Liao, S-Yi Fang and A. Chiang, *Adsorption*, 2010, **16**, 69.
15. X. Xu, J. Wang and Y. Long, *Sensors*, 2006, **6**, 1751.
16. K. Sahner, G. Hagen, D. Schönauer, S. Reiß and R. Moos, *Solid State Ionics*, 2008, **179**, 2416.
17. Y. Zheng, X. Li and P. K. Dutta, *Sensors*, 2012, **12**, 5170.
18. L. D. Bonifacio, B. V. Lotsch, D P. Puzzo, F. Scotognella and G. A. Ozin, *Adv. Mater.*, 2009, **21**, 1641.
19. J. Kobler, B. V. Lotsch, G. A. Ozin and T. Bein, *ACS Nano*, 2009, **3**, 1669.

20. B. V. Lotsch, F. Scotognella, K. Moeller, T. Bein and G. A. Ozin, Proc. of SPIE., V, 2010, **7713**, 77130.
21. F. M. Hinterholzinger, A. Ranft, J. M. Feckl, B. Ruhle, T. Bein and B. V. Lotsch, J. Mater. Chem., 2012, **22**, 10356.
22. T. Babeva, R. Todorov, B. Gospodinov, N. Malinowski, J. El Fallah and S. Mintova, J. Mater. Chem., 2012, **22**, 18136.
23. B. Gospodinov, J. Dikova, S. Mintova and T. Babeva, J. Phys. Conf. Ser., 2012, **398**, 1742.
24. S. Mintova, J.-P Gilson and V. Valtchev, Nanoscale, 2013, **5**, 6693.
25. S. Mintova and T. Bein, Micropor. Mesopor. Mat., 2001, **50**, 159.
26. S. Mintova and T. Bein, Adv. Mater., 2001, **13**, 1880.
27. A. M. Doyle, G. Rupprechter, N. Pfander, R. Schogl, C. E. A. Kirschlock, J. A. Martens and H. J. Freund, Chem. Phys. Lett., 2003, **382**, 404.
28. J. Kobler, H. Abrevaya, S. Mintova and T. Bein, J. Phys. Chem. C, 2008, **112**, 14274.
29. I. Yordanov, R. Knoerr, V. De Waele, M. Mostafavi, Ph. Bazin, S. Thomas, M. Rivallan, L. Lakiss, T.H. Metzger and S. Mintova, J. Phys. Chem. C, 2010, **114**, 20974.
30. M. Hölzl, S. Mintova and T. Bein, Stud. Surf. Sci. Catal., A, 2005, **158**, 11.
31. S. Mintova, N. H. Olson, J. Senker and T. Bein, Angew. Chem., 2002, **41**, 2558.
32. L. Lakiss, I. Yordanov, G. Majano, T. Metzger and S. Mintova, Thin Solid Films, 2010, **518**, 2241.
33. M.M. J. Treacy, J.B. Higgins and R. Ballmoos, Collection of Simulated XRD Powder Patterns for Zeolites, Elsevier, NewYork, 1996.
34. D. Bruggeman, Phys., 1935, **24**, 636.
35. T. Babeva, R. Todorov, S. Mintova, T. Yovcheva, I. Naydenova and V. Toal, J. Opt. A: Pure Appl. Opt., 2009, **11**, 024015.
36. E. Leite, T. Babeva, E.-P. Ng, V. Toal, S. Mintova and I. Naydenova, J. Phys. Chem. C, 2010, **114**, 16767.
37. Paulick, Handbook of Optical Constants of Solids, Academic, New York, 1985.
38. <http://www.raacke.de/index.html?airy.html>

39. H.-T Hsu, C.-Y. Ting, C.-Y. Mou and B.-Zu Wan, *Studies in Surface Science and Catalysis*, 2003, **146**, 539.
40. K. Lazarova, M. Vasileva, G. Marinov and T. Babeva, *Optics & Laser Technology*, 2014, **58**, 114.
41. M. E. Calvo and H. Míguez, in *Responsive Photonic Nanostructures: Smart Nanoscale Optical Materials*, ed. Yadong Yin, The Royal Society of Chemistry, Cambridge, UK, 2013, pp. 1-21.

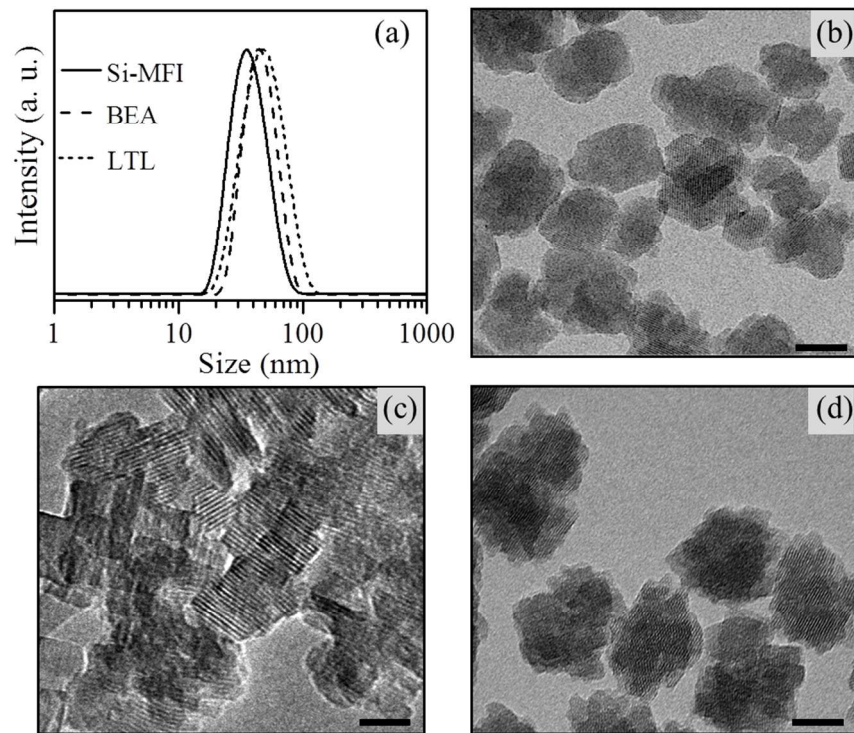


Figure 1. (a) DLS curves for colloidal suspensions containing Si-MFI, BEA and LTL type zeolites; TEM images of (b) Si-MFI and (c) LTL and (d) BEA zeolites ($M=20$ nm).

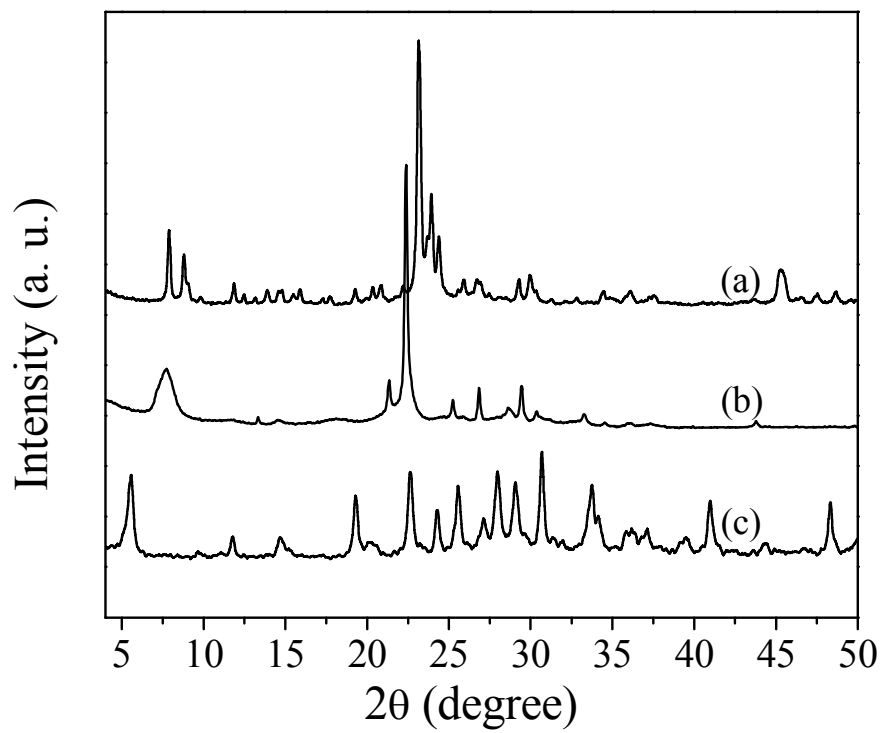


Figure 2. X-ray diffraction patterns of (a) Si-MFI, (b) BEA and (c) LTL powder samples.

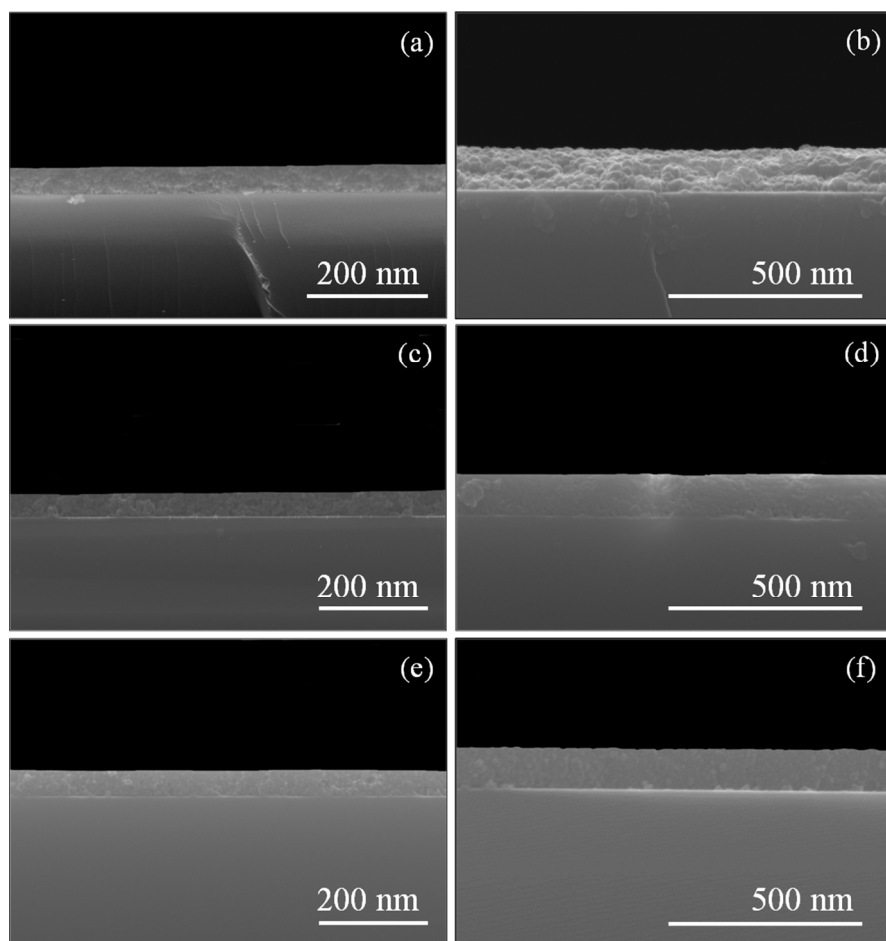


Figure 3. SEM images of zeolite films with the corresponding thickness of (a) Si-MFI-70 nm, (b) Si-MFI-150 nm, (c) BEA-70 nm, (d) BEA-150 nm, (e) LTL-70 nm, and (f) LTL-150 nm.

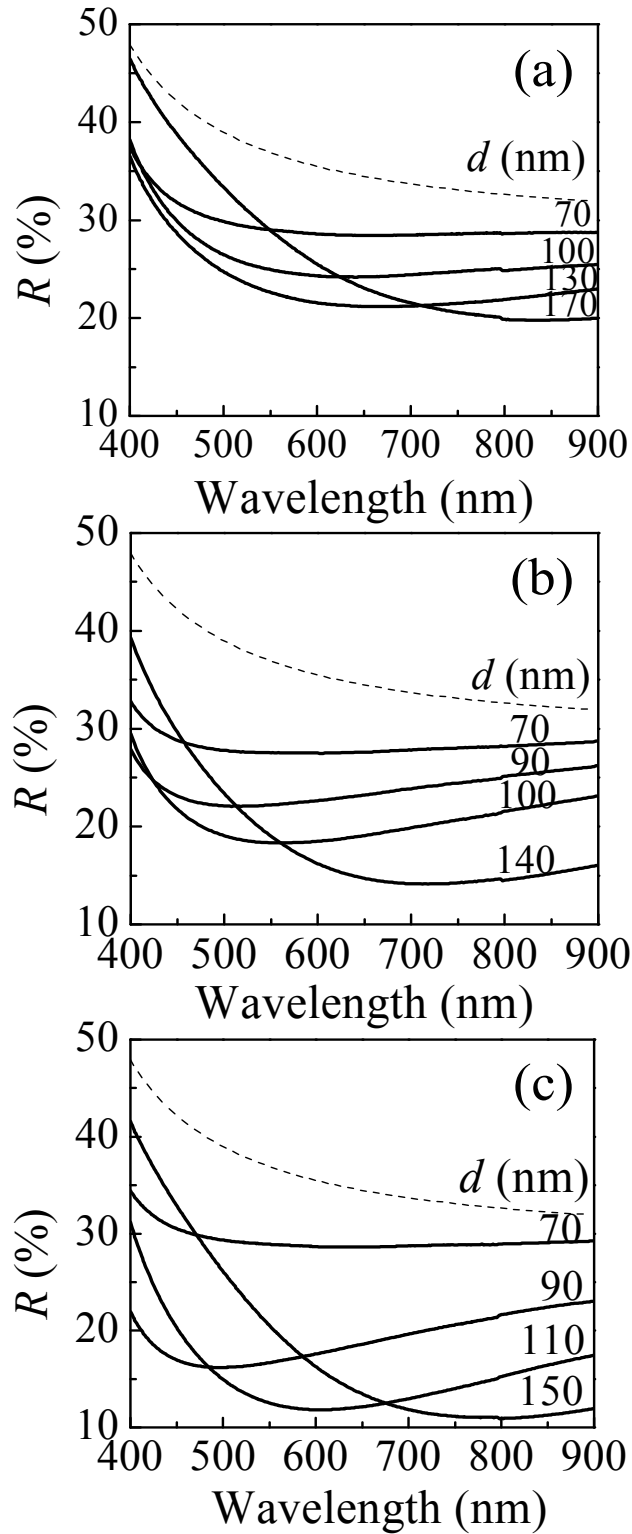


Figure 4. Reflectance spectra of (a) Si-MFI, (b) BEA and (c) LTL zeolite films deposited on Si substrates (the thicknesses of the films are denoted). The dashed curves correspond to the reflectance spectra of bare silicon wafer

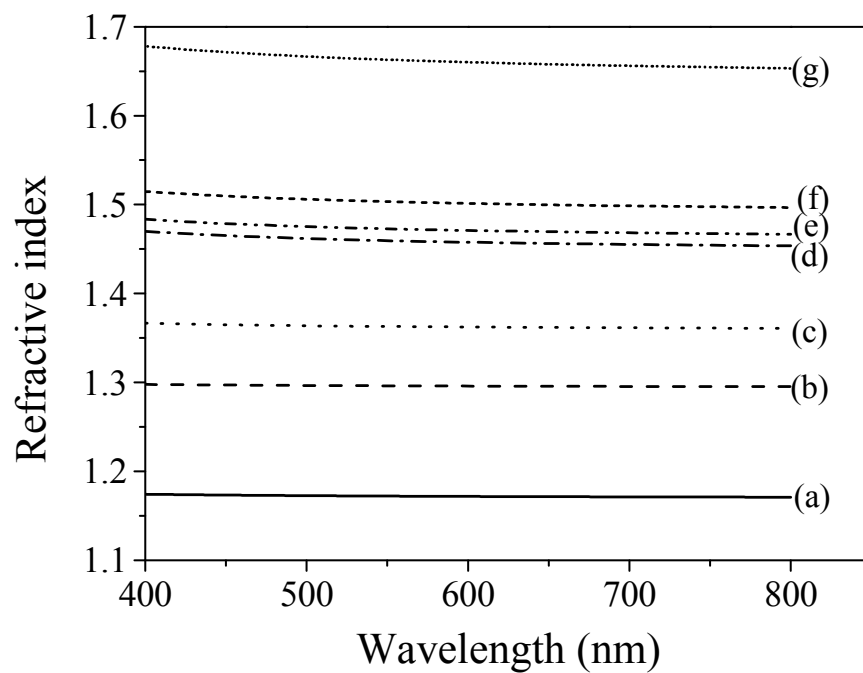


Figure 5. Calculated dispersion curves of refractive index for (a) Si-MFI, (b) BEA and (c) LTL films based on the measured reflectance spectra. Refractive index for SiO_2 (d) and Al_2O_3 (g) are taken from Ref. ³⁷. Calculated effective refractive index of media consisting of SiO_2 and Al_2O_3 in volume fractions that correspond to the Si/Al ratio of (e) 14, and (f) 3.6 using Bruggeman effective medium theory³⁴⁻³⁶

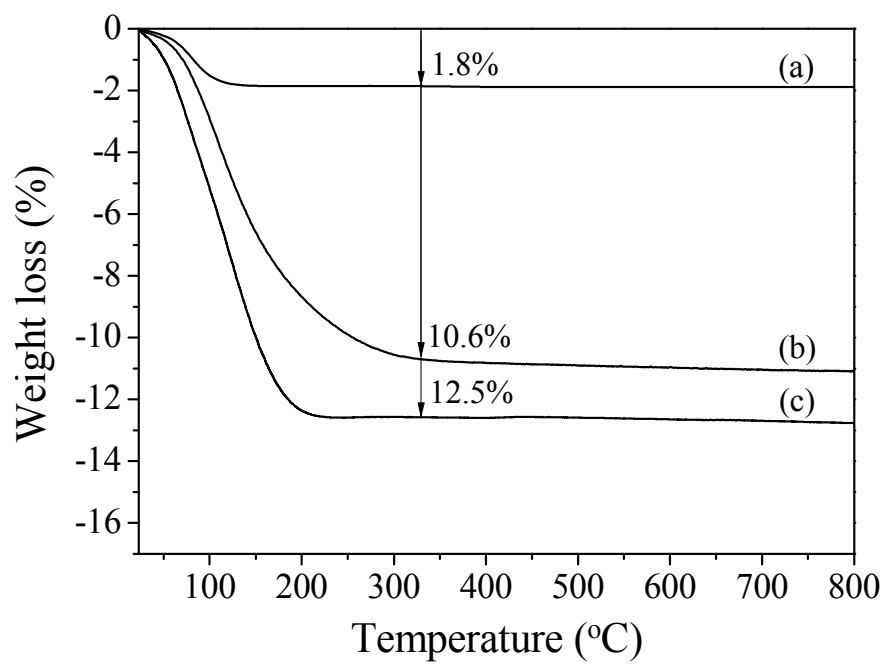


Figure 6. TG analysis of annealed (a) Si-MFI, (b) BEA and (c) LTL type zeolites.

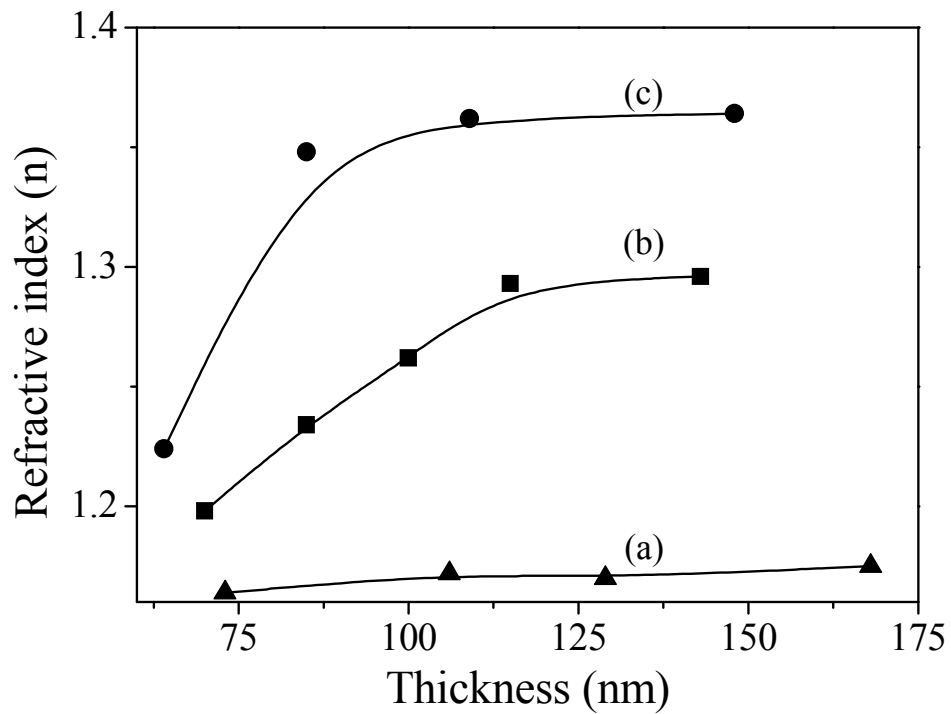


Figure 7. Thickness dependence of the refractive index (n) measured at 600 nm for (a) Si-MFI, (b) BEA and (c) LTL type zeolites.

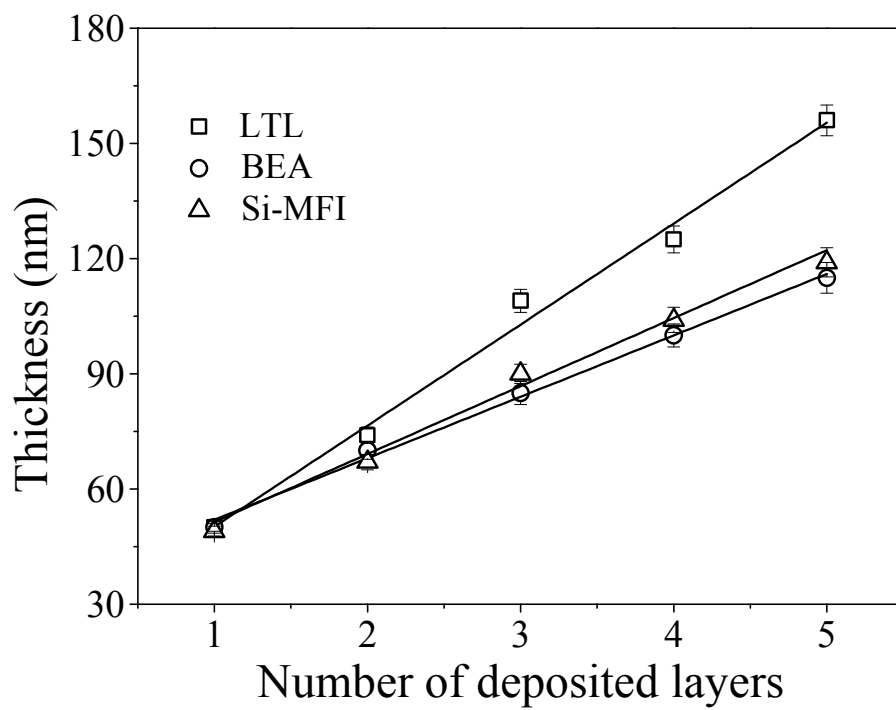


Figure 8. Thickness of zeolite films as a function of the number of deposition steps.

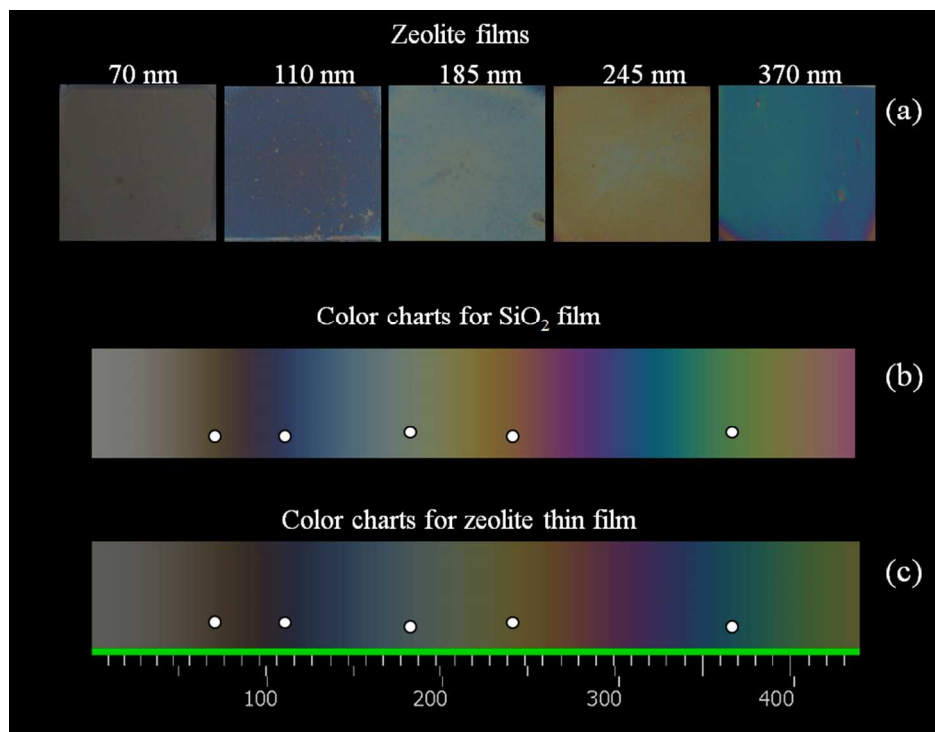


Figure 9. (a) Pictures of zeolite films deposited on Si-substrate by spin-coating method (thicknesses are denoted), (b) color charts of thermally grown SiO₂ films, and (c) the proposed color chart for zeolite films; (b, c) are generated from.³⁸

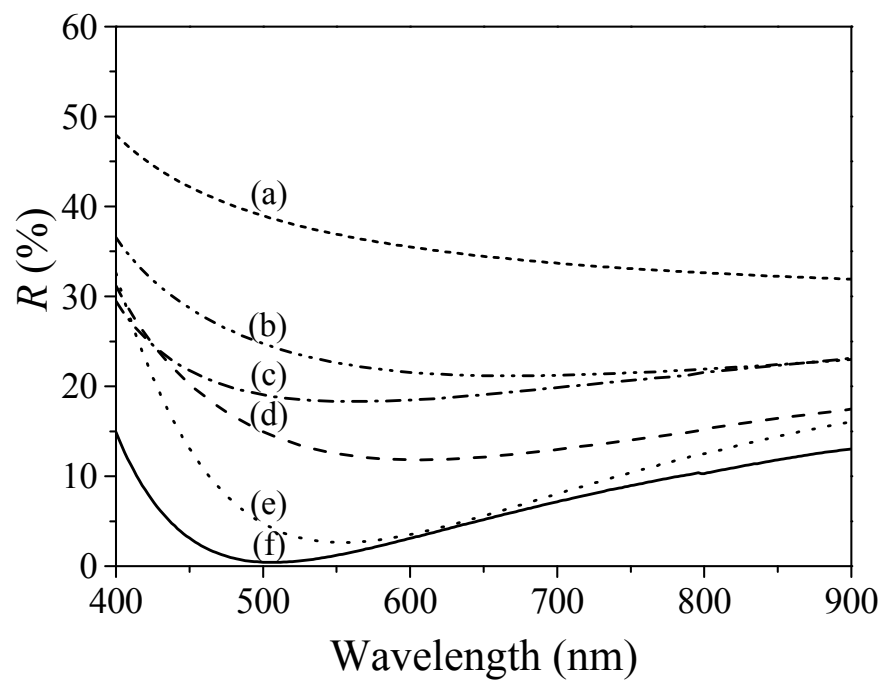


Figure 10. Reflectance spectra of (a) bare silicon substrate, and single AR coatings of (b) Si-MFI, (c) BEA and (d) LTL zeolites films with thickness of 120, 115 and 110 nm, respectively, (e) Nb₂O₅ film with thickness of 60 nm, and (f) stacks' AR coating consisting of Nb₂O₅ film (60 nm) and Si-MFI film (120 nm) on top of it.

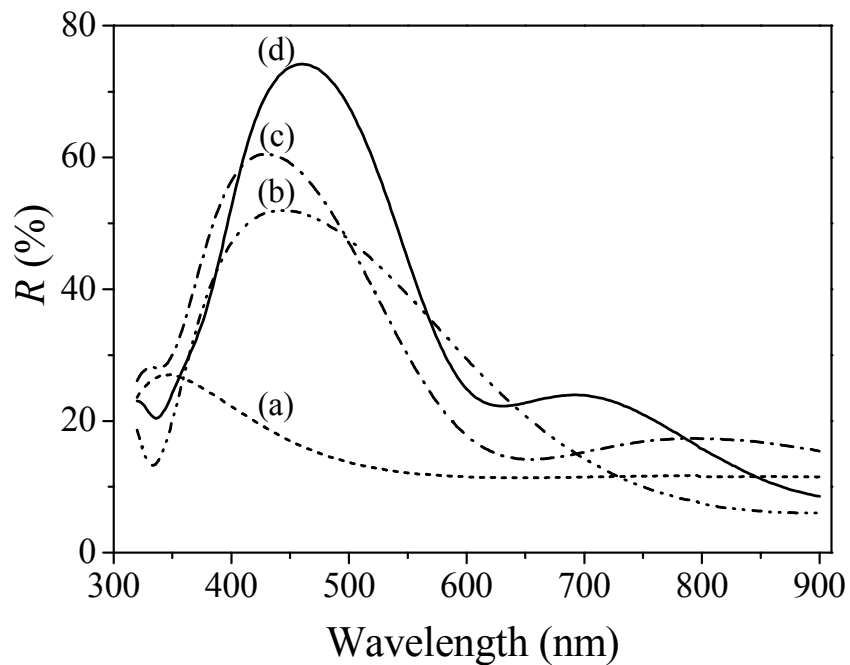


Figure 11. Reflectance band at normal incidence for (a) two, (b) three, (c) five, and (d) seven alternating films of Nb_2O_5 and Si-MFI deposited on glass substrate. The first film deposited on the glass substrate is Nb_2O_5 .

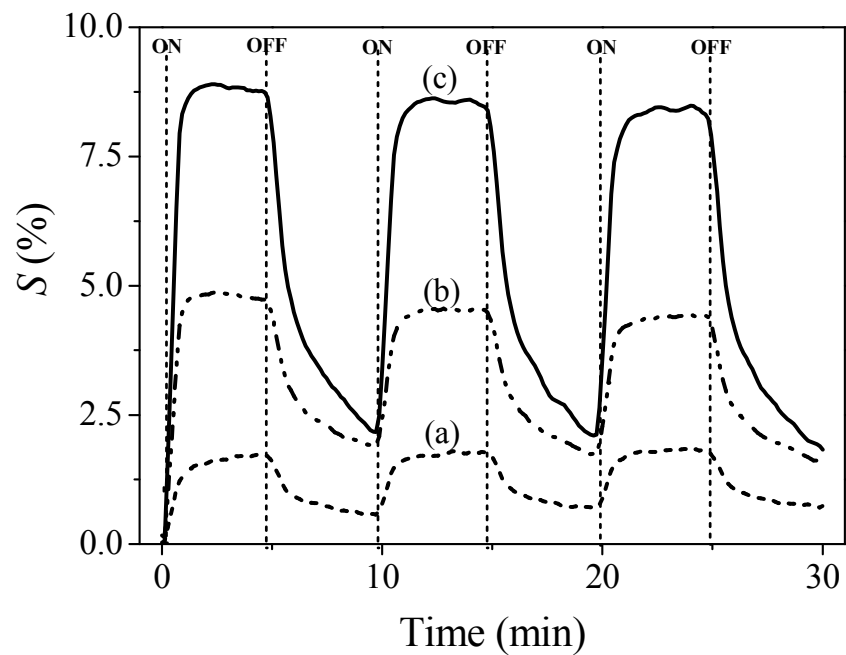


Figure 12. The transmittance signal (S) measured at wavelength of 400 nm for stacks comprising (a) three, (b) five and (c) seven alternating films of Nb_2O_5 and Si-MFI zeolite within 3 cycles of adsorption and desorption of acetone.

Optical properties of zeolite films and their applications in broadband antireflection coatings and Bragg stacks sensors.

